miR-191 promotes radiation resistance of prostate cancer through interaction with *RXRA*

Jessica Ray, Charles Haughey, Christianne Hoey, Jouhyun Jeon, Ross Murphy, Lara Dura-Perez, Nuala McCabe, Michelle Downes, Suneil Jain, Paul C. Boutros, Ian G. Mills, Stanley K. Liu

PII: S0304-3835(19)30639-1

DOI: https://doi.org/10.1016/j.canlet.2019.12.025

Reference: CAN 114621

To appear in: *Cancer Letters*

Received Date: 26 August 2019

Revised Date: 16 December 2019

Accepted Date: 19 December 2019

Please cite this article as: J. Ray, C. Haughey, C. Hoey, J. Jeon, R. Murphy, L. Dura-Perez, N. McCabe, M. Downes, S. Jain, P.C Boutros, I.G Mills, S.K Liu, miR-191 promotes radiation resistance of prostate cancer through interaction with *RXRA*, *Cancer Letters*, https://doi.org/10.1016/j.canlet.2019.12.025.

ABSTRACT

Radiation therapy is a common treatment for prostate cancer, however recurrence remains a problem. MicroRNA expression is altered in prostate cancer and may promote therapy resistance. Through bioinformatic analyses of TCGA and CPC-GENE patient cohorts, we identified higher miR-191 expression in tumor versus normal tissue, and increased expression in higher Gleason scores. *In vitro* and *in vivo* experiments demonstrated that miR-191 overexpression promotes radiation survival, and contributes to a more aggressive phenotype. Retinoid X receptor alpha, *RXRA*, was discovered to be a novel target of miR-191, and knockdown recapitulated radioresistance. Furthermore, treatment of prostate cancer cells with the *RXRA* agonist 9-*cis*-retinoic acid restored radiosensitivity. Supporting this relationship, patients with high miR-191 and low RXRA abundance experienced quicker biochemical recurrence. Reduced *RXRA* translated to a higher risk of distant failure after radiotherapy. Notably, this miR-191/*RXRA* interaction was conserved in a novel primary cell line derived from radiorecurrent prostate cancer. Together, our findings demonstrate that miR-191 promotes prostate cancer survival after radiotherapy, and highlights retinoids as a potential option to improve radiotherapy response.

miR-191 promotes radiation resistance of prostate cancer through interaction with *RXRA*

Jessica Ray[1,2], Charles Haughey[3], Christianne Hoey[1,2], Jouhyun Jeon[4], Ross Murphy[3], Lara Dura-Perez[3], Nuala McCabe[3], Michelle Downes[5], Suneil Jain[3], Paul C Boutros[2,4], Ian G Mills[3,6], Stanley K Liu[1,2,7].

[1]Sunnybrook Research Institute, Sunnybrook Health Sciences Centre, Toronto, Canada, [2]Department of Medical Biophysics, University of Toronto, Canada, [3]Centre for Cancer Research and Cell Biology, Queen's University Belfast, Northern Ireland, UK, [4]Ontario Institute for Cancer Research, Toronto, Canada, [5]Department of Anatomic Pathology, University of Toronto, Canada, [6]Nuffield Department of Surgical Sciences, University of Oxford, UK, [7]Department of Radiation Oncology, University of Toronto, Canada.

Corresponding author:
Dr. Stanley K Liu
2075 Bayview Avenue, Rm T2-169
Sunnybrook Health Sciences Centre
Toronto, Ontario, M4N 3M5
Phone: (416) 480-4998
Fax: (416) 480-6002
Email: stanley.liu@sunnybrook.ca

Conflict of Interest Statement: No conflicts of interest.

ABSTRACT

Radiation therapy is a common treatment for prostate cancer, however recurrence remains a problem. MicroRNA expression is altered in prostate cancer and may promote therapy resistance. Through bioinformatic analyses of TCGA and CPC-GENE patient cohorts, we identified higher miR-191 expression in tumor versus normal tissue, and increased expression in higher Gleason scores. *In vitro* and *in vivo* experiments demonstrated that miR-191 overexpression promotes radiation survival, and contributes to a more aggressive phenotype. Retinoid X receptor alpha, *RXRA*, was discovered to be a novel target of miR-191, and knockdown recapitulated radioresistance. Furthermore, treatment of prostate cancer cells with the *RXRA* agonist 9-*cis*-retinoic acid restored radiosensitivity. Supporting this relationship, patients with high miR-191 and low RXRA abundance experienced quicker biochemical recurrence. Reduced *RXRA* translated to a higher risk of distant failure after radiotherapy. Notably, this miR-191/*RXRA* interaction was conserved in a novel primary cell line derived from radiorecurrent prostate cancer. Together, our findings demonstrate that miR-191 promotes prostate cancer survival after radiotherapy, and highlights retinoids as a potential option to improve radiotherapy response.

Keywords: microRNA; microRNA-191; RXRA; radiation resistance; primary prostate cancer

1. INTRODUCTION

Radiation resistance in prostate cancer (PCa) remains a clinical problem. Although technological advances with radiotherapy planning and treatment delivery have facilitated dose escalation and hypofractionated treatment schedules, these have not translated to improved overall survival for patients[1]. In contrast, the addition of androgen-deprivation therapy has been demonstrated to improve overall survival, highlighting the importance of elucidating molecular mechanisms for radiation resistance[2]. By understanding the specific cellular mediators of resistance, we will ultimately be able to derive strategies for identifying patients likely to recur following treatment, and highlight new methods to improve patient outcomes following radiotherapy.

The aim of studying microRNAs (miRNAs) in the radiation setting is two-pronged: to describe their underlying biological mechanisms influencing sensitivity and use miRNAs as biomarkers to identify patients likely to recur following radiotherapy. miRNAs are a class of non-coding RNA molecules which are canonically negative regulators of gene abundance, through translation inhibition and mRNA degradation[3]. Several miRNAs have been shown to influence radiation sensitivity through regulation of various radiobiological processes, including DNA damage repair, hypoxia response, and survival signaling pathways[4, 5].

microRNA-191 (miR-191) has been identified as an important oncogenic miRNA in breast cancer, interacting with estrogen to promote tumorigenicity[6, 7]. The expression of miR-191 in cancer is often reported to be upregulated with advanced stage or compared with normal tissue, including in breast, colon, lung, pancreas, and stomach cancers[8, 9]. High throughput arrays have shown miR-191 expression may be induced by radiation treatment[10, 11], but no studies focusing on radiation survival effects of miR-191 have been reported.

In this study, the primary objective was to elucidate the role of miR-191 in PCa aggression and radiation response. Bioinformatic analyses of the TCGA and CPC-GENE datasets demonstrated that miR-191 is elevated in tumors versus matched normal prostates, and higher abundance is associated with higher Gleason score. Elevation of miR-191 in PCa cell lines conferred radiation resistance *in vitro* and *in vivo*, through interaction with a novel target, retinoid X receptor alpha (*RXRA*), a nuclear receptor for retinoids. Reduced *RXRA* expression was associated with a higher risk of distant relapse following radiotherapy in the Belfast cohort. In a novel primary PCa cell line derived from a patient with locally-recurrent disease, we confirmed that ectopic expression a miR-191 mimic or knockdown of RXRA induces radioresistance. Treatment with the retinoid 9-*cis*-retinoic acid resulted in radiosensitization, indicating that modulators of RXR activity may provide a therapeutic option for radioresistant PCa.

2. MATERIALS AND METHODS

2.1 Patient Analysis

The Cancer Genome Atlas (TCGA) prostate cohort contains data from 487 prostate cancer samples and 52 normal samples[12]. Of the tumor samples, 45 are Gleason 6(3+3), 144 are Gleason 7(3+4), 98 are Gleason 7(4+3), and 200 are Gleason >7. The Canadian Prostate Cancer Genome Network (CPC-GENE) dataset comprises 158 samples, of which 12 are Gleason 6, 137 are Gleason 7 (3+4 = 97 & 4+3 = 37), and 12 are Gleason >7[13]. Differential expression between multiple groups was evaluated using one-way ANOVA tests, and Student's t-test used for comparisons between two groups. All statistical analyses were completed using R statistical environment (v3.4.0). Cut-off of high/low expression was determined using cutP to find appropriate cutoffs to determine differences of survival between two groups.

The Belfast cohort consists of 248 prostate cancer patients with localized/locally advanced prostate cancer patients treated with radical radiotherapy (with/without ADT) at the NI Cancer Centre, Belfast Health and Social Care Trust (BHSCT), between 1 January 2005 and 31 December 2009 [14].

2.2 Cell Culture

Human prostate carcinoma cell lines DU145 and PC3 were purchased from American Type Culture Collection (ATCC), and maintained in Dulbecco's modified Eagle's medium containing 4.5 g/L D-glucose and GlutaMAX (DMEM; Gibco) supplemented with 10% FBS and 1% Penicillin-Streptomycin. All cell lines were maintained in tissue-culture flasks within a humidified 37°C incubator with 5% CO2, and passaged when they reached 80% confluency. Cell lines were regularly confirmed to be free from mycoplasma contamination using MycoAlert Detection Kit (Lonza).

2.3 hPCA9 Cell Culture Derivation

Primary prostate culture derivation was performed as previously described by *Frame et al*[15]. Fresh biopsy cores were obtained with ethical consent from the NI Biobank[16] from a patient with locally recurrent prostate cancer 8 years post definitive hypofractionated radiotherapy and bicalutamide treatment (for in depth patient characteristics see Table I). Briefly, 7.5mL of filtered collagenase solution (Worthington Biochemicals) [consisting of 5mL RPMI with 10% FBS, and 2.5mL KSFM] at a final concentration of 200IU/mL, was added to the tissue before using a sterile scalpel to mechanically chop the tissue into 1mm pieces. Tissue suspension was then transferred to a 50mL falcon tube and incubated over night at 37ºC in an orbital shaker at 80rpm. The following day, the collagenase/tissue solution was passed through a blunt needle several times before being centrifuged at 380xg for 5 minutes. The pellet was then washed twice with 1X PBS to remove any remaining collagenase before resuspending in 10mL of 1X trypsin and incubating for 30mins at 37º C in an orbital shaker at 80rpm. 10mL of RPMI 10% FBS was added to the trypsin/cell solution and vigorously shaken prior to being centrifuged at 380xg for 5mins. The pellet was then washed with 1X PBS to remove any remaining RPMI 10% FBS and resuspended in 6mL SCM media [SCM: KSFM (Thermo Fisher) with epidermal growth factor, bovine pituitary extract, 1ng/mL GM-CSF (Miltenyi Biotec), 2ng/mL stem cell factor (Stem cell technologies), 2ng/mL leukaemia inhibitory factor (merckmillipore) and

100ng/mL cholera toxin (Sigma)]. The cell suspension was then plated onto a type 1 collagen coated plate (Corning BioCoat) with Mitomycin C (Sigma) treated STO cells. Colonies were seen within 10-14 days.

2.4 Immortalization of primary culture

Production of the lentivirus containing the vector coding for SV40 large T unit gene was performed as per manufacturer instructions (Thermo Fisher). Sub-confluent hPCA9 cultures were plated on type 1 collagen plate and allowed to adhere for 24 hours, after which cultures were infected with lentivirus supernatants for 12 hours. Viral media on the cultures was then replaced with fresh SCM. hPCA9 cultures were serially passaged to ensure replication capacity of the cell line.

2.5 Mimics, siRNAs and Transfection

DU145, PC3, or hPCA9 cells were seeded in a 6-well plate, and transfected for 24 hours using Lipofectamine 2000 (Invitrogen) according to manufacturer's specifications. Negative control and miR-191 (miR-191-5p) mimics were obtained from Shanghai GenePharma Co., while pooled RXRA and control siRNA were purchased from Santa Cruz Biotechnology (Catalog numbers and sequences in Supplementary Table I). All RNA products were reconstituted in RNAse-free water and stored at -80°C.

2.6 Quantitative real-time PCR (qRT-PCR)

For quantifying miRNA abundance, total mRNA was extracted using the miRVana miRNA isolation kit as per the manufacturer's instructions (Life Technologies), followed by synthesis of cDNA using the miScript II RT kit (Qiagen). qRT-PCR was performed on a StepOnePlus Real-Time PCR system (Applied Biosystems) with miScript SYBR Green PCR kit and miScript Primer Assays for RNU6 and miR-191-5p both purchased from Qiagen (RNU6 cat. no.: MS00033740; miR-191-5p: MS00003682). For mRNA expression, total RNA was collected using the RNeasy Mini Kit (Qiagen), and cDNA generated with the Superscript VILO cDNA kit (Thermo Fisher Scientific). SYBR Select Master Mix (Applied Biosystems) was used for qRT-PCR, along with primers designed using Primer-BLAST software (NCBI) and synthesized by Invitrogen. Abundance was calculated with the comparative Ct method using StepOne Software (Applied Biosystems), and relative expression normalized to RNU6 for miRNA or GADPH for mRNA. All primer sequences available in Supplementary Table II.

2.7 Clonogenic Survival Assay

Cells were plated in triplicate in 6-well plates and mock irradiated (0 Gy) or treated with a 2, 4, 6, or 8 Gy dose of ionizing radiation (IR). For clonogenic assays testing 9-*cis*-retinoic acid (9cRA), transfected cells were seeded as per other clonogenics, then treated with 9cRA [DU145 = 1µM, hPCA9 = 0.1µM] (Sigma) or DMSO the following day. The plates were pre-treated with drug for 24 hours, then irradiated without changing media. For all clonogenics, plates were incubated for 10-14 days to allow for colony formation, and then stained using crystal violet (Sigma). Number of colonies were counted (defined as >50 cells), and surviving fraction of irradiated cells calculated relative

to plating efficiency of mock irradiated cells. Radiation dose response curves were generated by fitting the surviving fraction data to the linear quadratic formula $S = e^{-\alpha D-\beta D2}$.

2.8 Proliferation Assay

Cells were seeded in triplicate in 6-well plates at 1 x 10^5 cells per well or 5 x 10^4 cells per well for irradiation (6 Gy) and mock irradiation (0 Gy) respectively. After incubation for 4 days (0 Gy) or 5 days (6 Gy) post-treatment, wells were trypsinized and total viable cells determined using trypan blue exclusion on a Countess automated cell counter (Invitrogen). Results are expressed as fold change in number of cells from seeding to counting.

2.9 Cell Cycle Analysis

DU145 or PC3 cells were seeded in a 6-well plate and the following day transfected with mimics or siRNA. 24 hours after transfection, the cells were irradiated (10Gy) then incubated undisturbed for 24 hours, at which time they were fixed and stained as previously described[17]. EdU and DAPI or 7-AAD staining using the Click-iT EdU kit (Thermo Fisher) was performed as per manufacturer's specifications 24 hours following irradiation or mock irradiation. Samples were run using a FACSCalibur flow cytometer (BD Biosciences), and cell cycle profile was generated using FlowJo software (Version 10.0.4; FlowJo LLC).

2.10 Transcriptomic Analysis

Total RNA from transfected DU145 cells was extracted using RNeasy Mini Kit (Qiagen), and RNA quality assessed using a spectrophotometer. Samples were ethanol precipitated if found to have an 260nm absorbance ≤ 1.8. Gene expression profiling was performed by the Centre for Applied Genomics (The Hospital for Sick Children, Toronto, Canada) using a GeneChip Human Gene 2.0 ST array (Affymetrix). Transcriptomic data was normalized using Expression Console software (V.1.2, Affymetrix).

2.11 *In silico* analysis

Targets of miR-191 were identified *in silico* using miRWalk 2.0, which combines predicted and experimentally validated microRNA targets from 12 different miRNA-target prediction algorithms[18].

2.12 3'UTR Luciferase Assay

A wild-type RXRA 3'UTR luciferase reporter or the a mutated RXRA 3'UTR reporter with predicted miR-191 binding site sequence 5'-TTCCGTT-3' mutated to 5'-AAGGCAA-3' were obtained from ABMGood. DU145 cells were triple transfected with wild-type or mutated RXRA 3'UTR luciferase reporter and control or miR-191 mimic, with Renilla luciferase plasmid. 48 hours after transfection, Firefly and Renilla luciferase activity was measured using the Dual Glo Luciferase assay system (Promega). Reporter Firefly luciferase was normalized to Renilla luciferase activity to account for transfection efficiency.

2.13 Western Blotting

48 hours after mimic or siRNA transfection, cells were rinsed with PBS and lysed in ice-cold RIPA lysis buffer containing Complete Mini protease inhibitor cocktail and PhosSTOP phosphatase inhibitor cocktail (Roche Diagnostics). Protein lysate was run on a 4-20% polyacrimide gradient gel (Bio-Rad), wet-transferred to polyvinylidene difluoride membranes (Thermo Fisher Scientific), and blocked for 1 hour with either 5% non-fat dry milk or 5% bovine serum albumin (BSA). Primary antibody in appropriate solution (5% milk or 5% BSA) was added and incubated overnight at 4°C, then incubated with horseradish peroxidase-conjugated anti-rabbit IgG secondary antibody (1:5000) for 1 hour at room temperature. The following antibodies from Cell Signaling Technologies were used: β-actin (1:2000, anti-rabbit), RXRA (1:1000, anti-rabbit).

2.14 *In vivo* tumor xenograft studies

All experiments involving animals were performed in accordance with University of Toronto and Sunnybrook Research Institute Animal Care Committee guidelines using a peer-reviewed protocol. Six to seven week old female athymic nude mice (Charles River) were injected subcutaneously into the right flank with 3 million DU145 control-st or miR-191-st cell lines mixed 1:1 (v/v) with Matrigel (Corning). When tumor volumes reached an average of 100mm^3, mice were randomized to receive mock ionizing radiation (IR) or 6Gy IR. Mice were monitored every 2-3 days and tumors measured using calipers. Tumor volume was calculated using the modified ellipsoid formula: volume = ½ (length x width^2). Endpoint defined as 2X starting volume.

2.15 Immunohistochemistry

Xenograft sections cryopreserved in Tissue-Tek O.C.T (Fisher Scientific) were processed into 5µM thick sections and stained for hematoxylin and eosin (H&E) or Ki-67. Areas of necrosis were quantitated using ImageJ software, and necrosis as a percentage of total tumor area graphed (n=5 tumors per group), while Ki-67 evaluated by manual counting of 5 representative areas imaged under 40X magnification power (n=3 tumors per group). .

2.16 Statistical Analyses

Statistical analyses were performed using GraphPad Prism 5.0 (GraphPad Software), except for analyses conducted on patient samples which were performed in R. All experiments consist of at least three experimental replicates, unless otherwise noted. Differences in means were compared using two-sided Student's *t*-test, and graphed as mean with SEM. Statistical significance denoted as *p<0.05, **p<0.01, ***p<0.001.

3 RESULTS

3.1 miR-191 abundance is elevated in prostate cancer

To determine the significance of miR-191 in prostate cancer (PCa), we analyzed miRNA abundance in The Cancer Genome Atlas (TCGA) prostate dataset[12]. This revealed that miR-191 abundance was significantly higher in PCa when compared to normal prostate tissue (Fig. 1A). Moreover, when stratifying PCa by Gleason score, miR-191 abundance was significantly elevated with increasing Gleason score (Fig. 1B). Using follow-up data from the CPC-GENE cohort, we identified an association between high miR-191 expression and time to relapse, amongst patients who experienced biochemical relapse (BCR) (Fig. 1C). Together these data provide evidence that miR-191 is increased in PCa, particularly high grade disease, and is a candidate biomarker for biochemical relapse.

3.2 miR-191 promotes radiation resistance

In order to evaluate the effects of miR-191 *in vitro*, we transfected two human PCa cell lines (DU145 and PC3) with miR-191 or control mimic, and verified the overexpression of miR-191 using qRT-PCR (Supplementary Figure 1A). We then performed radiation clonogenic survival assays in both DU145 and PC3 cell lines, which revealed miR-191 overexpression significantly increased radiation survival compared to a control mimic (Fig. 2A). We observed a significant increase in the number of viable DU145 cells after 6Gy irradiation in the miR-191 mimic population, compared with control mimic (Fig. 2B). In addition, there was a non-significant decrease in the number of viable DU145 cells overexpressing miR-191 versus control cells prior to irradiation. Consistent with this, cell cycle analysis demonstrated a significant reduction in S-phase of non-irradiated miR-191 DU145 cells compared to control (Fig. 2C, left panel). Following irradiation, there was no difference seen in S-phase, however a reduced G2-M was noted in miR-191 cells (Fig. 2C, right panel), likely contributing to the increased survival observed in clonogenic experiments. Transfection of PC3 cells with miR-191 mimic significantly reduced the number of viable cells compared to control mimic (Fig. 2D), which corresponded with a significant reduction in S-phase in the miR-191 population in the cell cycle analysis (Fig. 2E, left panel). After irradiation, this difference in viable cells was no longer observed, indicating that miR-191 promotes survival after irradiation. PC3 cell cycle profiles showed the miR-191 transfected cells demonstrated significantly lower G2-M block 24 hours after irradiation (Fig. 2E, right panel), supporting the radiation resistance effect observed. miR-191 effects on cell cycle profiles were similarly seen with EdU labelling experiments (Supplementary Figure 2).

3.3 *RXRA* is reduced by miR-191

To elucidate the mechanism of miR-191 radioresistance, we performed a transcriptomic analysis of DU145 cells transfected with miR-191 or control mimic, which we combined with an *in silico* prediction algorithm (miRwalk 2.0[18]) to identify putative miR-191 target genes (Fig. 3A). This generated 18 prospective target genes (Supplementary Table III), and we chose to focus on retinoid X receptor alpha (RXRA) due to the previous literature supporting retinoic acid in radiation response. RXRA is a nuclear receptor that mediates retinoic acid-mediated gene activation, and several publications had demonstrated that its agonist 9-*cis*-retinoic acid (9cRA) promotes cancer cell radiosensitivity[19, 20]. qRT-PCR and western blots confirmed that *RXRA* mRNA and protein was reduced with

miR-191 mimic transfection in DU145 and PC3 cells (Fig. 3B). Reporter constructs containing a region of the *RXRA* 3'UTR with either a wild-type (WT) miR-191 binding site, or a mutated (MT) miR-191 binding site were transfected with miR-191 or control mimic into DU145 cells and luciferase assays performed. Luciferase activity of WT vector with miR-191 mimic was reduced compared with control mimic, however MT luciferase activity remained unchanged (Fig. 3C). Collectively, these experiments established *RXRA* as novel, validated target gene of miR-191 in PCa.

3.4 RXRA is down-regulated in prostate cancer

We performed bioinformatics analyses using the same patient cohorts as miR-191, which revealed *RXRA* abundance is lower in PCa compared with normal tissue; inverse to the trend observed with miR-191 (Fig. 4A). In addition, biochemical relapse-free survival was faster in patients with low abundance *RXRA* (Fig. 4B). Combination of miR-191 and *RXRA* abundance data revealed that prostate tumors in the high miR-191, low *RXRA* group displayed the worst BCR, whereas low miR-191, high *RXRA* tumors have the greatest relapse-free survival at 5 years (Fig. 4C). These analyses support *RXRA* as a miR-191 target, and highlight a potential role for miR-191 upregulation along with *RXRA* reduction as a biomarker for poor prognosis. Accordingly, in a large Belfast cohort of localized and locally-advanced PCa patients treated with definitive radiotherapy[14], patients within the lowest quartile of *RXRA* abundance were at significantly greater risk of experiencing distant metastatic failure compared to patients with high *RXRA* (Fig. 4D).

3.5 *RXRA* knockdown increases radiation resistance

To demonstrate that reduction of *RXRA* expression can recapitulate radiation resistance, we used siRNA to knockdown *RXRA* expression in DU145 and PC3 cells, which was confirmed through qRT-PCR and western blotting (Supplementary Figure 1B). Clonogenic survival assays showed that *RXRA* knockdown significantly increased radiation survival in both cell lines (Fig. 5A). Proliferation of *RXRA* knockdown in DU145 and PC3 cells phenocopied the results seen with our miR-191 experiments (Fig. 5B).

9-*cis*-retinoic acid (9cRA) is an endogenous ligand for *RXRA*, and studies have previously demonstrated that it can radiosensitize cells *in vitro*[20]. In agreement with this finding, 24 hour pre-treatment with 9cRA significantly reduced radiation survival of DU145 cells transfected with control mimic, when compared with vehicle (DMSO) (Fig. 5C and Supplementary Figure 3). In contrast, we did not observe significant radiosensitization of miR-191 mimic transfected DU145 cells with 9cRA relative to vehicle (Fig. 5C). We hypothesize that as miR-191 lowers RXRA levels, this limits the radiosensitizing effect of its ligand, 9cRA. This supports the model of miR-191 radioresistance mediated through RXRA.

3.6 Validation of miR-191 and RXRA phenotypes in a primary prostate cancer cell line

PC3 and DU145 cell lines were originally derived from PCa patients with distant metastases (bone and brain, respectively), and hence their biology may not be entirely reflective of localized disease. Thus, a primary PCa cell line (hPCA9) was derived from a patient with locally recurrent PCa (detailed in materials and methods) and utilized

to evaluate the miR-191 and RXRA interaction in the context of localized disease. hPCA9 cells were transfected with mimics or siRNA, and transfection efficiency confirmed using qRT-PCR and western blotting (Supplementary Figures 1A&B). In agreement with the above, there was a significant reduction in RXRA following miR-191 mimic transfection relative to control (Supplementary Figure 1C). Both elevation of miR-191 and knockdown of RXRA in hPCA9 displayed a similar trend to the radioresistance observed in PC3 and DU145 cells (Fig. 5D). In addition, treatment with 9cRA significantly reduced the surviving fraction of cells after 6Gy, similar to the effect in DU145 cells (Fig. 5E).

3.7 miR-191 promotes radiation resistance *in vivo*

We next evaluated *in vivo* radiation resistance through tumor growth xenograft experiments. DU145 cells were chosen given that they are derived from adenocarcinoma, the most common histological type of PCa. We first generated DU145 cells with stable overexpression of miR-191 (miR-191-st) or control mimic (control-st) using lentivirus followed by antibiotic selection, and confirmed stable overexpression of miR-191 through qRT-PCR (Supplementary Figure 1D). In addition, we verified that miR-191-st cells had increased clonogenic survival and viability following radiation, relative to control-st cells (Fig. 6A).

Mice were injected subcutaneously with either control-st or miR-191-st cells, and randomly assigned to receive mock IR or 6Gy IR once average tumor volume reached approximately $100mm^3$. Mice bearing control-st or miR-191-st tumor xenografts randomized to mock irradiation displayed no significant differences in tumor growth, consistent with DU145 proliferation and cell cycle assays *in vitro* (Fig. 6B). The miR-191-st tumors treated with radiation reached the experimental endpoint (double the starting tumor volume) by approximately 54 days. In contrast, the irradiated control tumors did not demonstrate any regrowth by this time point. After tumors reached experimental endpoints, excised tumors were stained with H&E and examined for areas of necrosis. miR-191-st xenograft sections treated with IR displayed significantly less necrosis compared with the control-st IR treated tumors (Fig. 6C). Immunostaining for the proliferative marker Ki-67 showed significantly reduced Ki-67 positive cells in miR-191-st tumors relative to control-st tumors after IR (Fig. 6D), supportive of our *in vitro* findings.

4 DISCUSSION

Elucidating the role of miRNAs in prostate cancer (PCa) is key to understanding the molecular mechanisms underlying treatment resistance and for identifying avenues to overcome this challenge. For the first time, we have demonstrated the role of miR-191 in promoting radiation resistance, which is mediated in part through the novel miR-191 target retinoid X receptor alpha (RXRA). Knockdown of *RXRA* promotes radiation resistance in PCa cells, and re-sensitization can be achieved by treatment with the RXRA ligand 9-*cis*-retinoic acid (9cRA). In PCa patient cohorts, we demonstrated the prognostic ability of high miR-191 alone and in combination with low RXRA in highlighting patients with earlier disease recurrence.

The abundance of miR-191 is frequently elevated in tumor compared with normal tissue, such as in breast, hepatocellular, colon, lung, and pancreatic cancers[8, 9, 21]. Wang *et al.* recently reported that miR-191 is more abundant in human PCa tissue relative to benign tissue using a small cohort of PCa patients[22]. However, no outcome data was reported and thus correlation of miR-191 abundance with patient outcomes could not be determined. In a different study, Leite *et al.* identified that high miR-191 is associated with a higher risk of biochemical recurrence, using a small cohort of patients treated with radical prostatectomy[23]. Both of these previous studies in PCa support our own analysis using larger patient cohorts, in which miR-191 abundance was increased in tumors versus normal tissue and associated with increasing Gleason grade and faster time to biochemical relapse. However, based on our findings demonstrating a role for miR-191 in radiation response, patients treated with definitive radiotherapy would be the optimal cohort to examine miR-191 as a predictor of clinical outcome. However, there are currently no large datasets containing miRNA abundance derived from pre-radiotherapy PCa biopsies, and this this will be an important area of research for the future.

Several studies have identified miR-191 as highly abundant in patient tissue samples, and evaluated it as a potential endogenous normalization control for miRNA quantification experiments[24]. Based on our identification of differential normal versus tumor abundance in PCa, as well as previous studies demonstrating variable expression between normal and carcinoma samples[9], there is accumulating evidence that miR-191 plays a functional role in oncogenesis and its abundance can differ in disease.

The molecular contribution of miR-191 in oncogenesis has been best characterized in breast cancer, where multiple reports have indicated its importance in promoting invasion and proliferation in an estrogen responsive manner[6, 7, 25-27]. However, its functional role in PCa has not been well elucidated to date. To our knowledge, the report by Wang *et al*. represents the only published *in vitro* study, with no studies, to date, assessing radiation response or function *in vivo*[22]. In searching for miRNA that displayed altered abundance following ionizing radiation, Li *et al.* discovered that miR-191 was increased 3.3-fold in LNCaP PCa cells suggesting its potential role in radiation response[11]. However, no further experiments were conducted to specifically evaluate its role. We have now provided data that demonstrates the ability of miR-191 to promote radiation resistance. This is supported mechanistically by miR-191's effects on cell cycle distribution and proliferation, with a reduction in G2-M phase arrest post-radiation illustrating the ability of these cells to overcome growth arrest and continue cell division. Although we observed no significant difference in proliferation between control and miR-191 cells prior to

radiation, the miR-191 cells retained increased viability following irradiation relative to untreated proliferative capacity. We did not observe an increased proportion of miR-191 cells in S-phase prior or following radiotherapy, suggesting that

this least radiosensitive phase of the cell cycle is not contributing to radioresistance. Additionally, we evaluated resolution of γ-H2AX foci following irradiation and noted no significant differences in resolution between control and miR-191 mimic (Supplementary Figure 4). Thus, miR-191 does not promote radioresistance via increased S-phase population nor enhanced DNA double-stranded break repair.

Several miR-191 targets have been identified in various cancers, which is well summarized in a review by Nagpal *et al*[8]. We examined miR-191 effect on candidate targets that were previously reported in other cancer types, but did not observe a consistent decrease in their mRNA expression in PCa as evaluated by transcriptomic analyses and qRT-PCR (data not shown). However, it is known that miRNA target genes and molecular functions can be dependent on cancer type, tissue location, and genetic or epigenetic regulation within the cell[28, 29]. Through combining *in silico* predictions with our own transcriptomic data, we identified and validated *RXRA* as a novel target of miR-191 in PCa, through which radiation survival is promoted. Indeed, we discovered that reduced *RXRA* abundance results in a greater risk of distant metastatic failure following prostate radiotherapy.

RXRA is one of three retinoic X receptors (RXRs), a family of nuclear receptors which form homodimers as well as heterodimers with several other nuclear receptors including retinoic acid receptors (RARs). The role of retinoic acid receptors and ligands in cancer therapy have been explored since the 1990's, and therapeutic agonists targeting RARs and RXRs are being studied in cancer clinical trials[30]. Indeed, 9cRA has been postulated as a chemopreventive agent for PCa based upon its ability to decrease PCa development in a rat model using dietary 9cRA supplementation with no reported toxicity[31]. Additionally, IRX4204 was developed as a highly selective RXR agonist compound and a phase II clinical trial in men with metastatic castration-resistant PCa has shown progression-free survival responses of greater than 56 days in 57% of patients[32]. Many of these patients were heavily pre-treated (i.e., failed taxane chemotherapy) and IRX4204 was well tolerated, thus providing support for RXR agonists as a therapeutic avenue in advanced PCa.

Our work demonstrates that knockdown of RXRA promotes radiation survival, supporting miR-191/RXRA interaction as the mechanism of miR-191 induced radioresistance. The ability of the RXR agonist 9cRA, to radiosensitize PCa cells supports an important role of retinoic acid signaling in PCa radiation response. The radiosensitizing effect of 9cRA is non-significant in miR-191 overexpressing cells, and we hypothesize that this is due to reduced RXRA protein abundance, resulting in an attenuated effect of RXRA agonist treatment. This effect of RXRA abundance altering 9cRA efficacy has been demonstrated previously with apoptosis in a different PCa cell line[33].

Prostate cancer research has long been hindered by the lack of availability of *in vitro* models. Many of these models have been derived from metastatic lesions and therefore are not representative of the primary form of the disease. While other cancer fields, e.g. breast, have benefited from the increased use of primary cell lines to investigate novel drug targets, the PCa field has lagged as a result of primary tumor cell lines being notoriously hard to derive and maintain[15]. However even with these drawbacks, primary prostate cell lines offer advantages over other cell line

models as they are a closer representation of the heterogeneity of an individual patients tumor. The primary prostate cancer cell line, hPCA9, was derived from a local recurrence arising in a patient with previously treated disease, and thus represents a clinically relevant model of localized PCa. Using this model we further validated the miR-191/RXRA interaction as a mechanism for radiation resistance, and have shown that the RXRA agonist 9cRA induces radiation sensitivity in a primary PCa model.

In summary, we have demonstrated for the first time that miR-191 can promote radiation resistance *in vitro* and *in vivo* and its abundance in prostate cancer is increased in higher Gleason grade, and predicts for an earlier relapse-rate. Our discovery of the *RXRA*-9cRA axis as a target of miR-191 opens up a novel avenue for therapeutic intervention to improve radiation response.

AVAILABILITY OF DATA

All data generated or analyzed during the current study are included in this published article.

ACKNOWLEDGMENTS AND FUNDING SOURCES

The authors would like to thank the generous support provided by Prostate Cancer Canada. SKL is a Movember Rising Star award recipient proudly funded by the Movember Foundation (Grants # RS2014-03, #D2013-24, #D2015-12), the Telus Motorcycle Ride For Dad (Huronia Branch), and a Ministry of Research and Innovation Early Researcher Award. PCB is also supported by Prostate Cancer Canada and the Movember Foundation (Grant #RS2014-01). This study was conducted with the support of the Ontario Institute for Cancer Research to PCB through funding provided by the Government of Ontario, a Terry Fox Research Institute New Investigator Award, and a CIHR New Investigator Award. In addition the authors would like to sincerely thank the Gracey Foundation for their generous funding in support of this work.

The samples used in this research were received from the Northern Ireland Biobank which has received funds from HSC Research and Development Division of the Public Health Agency in Northern Ireland and the Friends of the Cancer Centre.

References

[1] J.M. Michalski, J. Moughan, J. Purdy, W. Bosch, D.W. Bruner, J.-P. Bahary, H. Lau, M. Duclos, M. Parliament, G. Morton, D. Hamstra, M. Seider, M.I. Lock, M. Patel, H. Gay, E. Vigneault, K. Winter, H. Sandler, Effect of Standard vs Dose-Escalated Radiation Therapy for Patients With Intermediate-Risk Prostate Cancer: The NRG Oncology RTOG 0126 Randomized Clinical TrialStandard vs Dose-Escalated Radiotherapy in Medium-Risk Prostate CancerStandard vs Dose-Escalated Radiotherapy in Medium-Risk Prostate Cancer, JAMA Oncology, 4 (2018) e180039-e180039.
[2] A. Pollack, M.C. Abramowitz, Weighing the Addition of Androgen Suppression Therapy to Radiotherapy Dose Escalation for Intermediate-Risk Prostate Cancer, J Clin Oncol, 34 (2016) 1715-1717.
[3] D.P. Bartel, MicroRNAs: genomics, biogenesis, mechanism, and function, Cell, 116 (2004) 281-297.
[4] E. Korpela, D. Vesprini, S.K. Liu, MicroRNA in radiotherapy: miRage or miRador?, British journal of cancer, 112 (2015) 777-782.
[5] C. Metheetrairut, F.J. Slack, MicroRNAs in the ionizing radiation response and in radiotherapy, Curr Opin Genet Dev, 23 (2013) 12-19.
[6] G. Di Leva, C. Piovan, P. Gasparini, A. Ngankeu, C. Taccioli, D. Briskin, D.G. Cheung, B. Bolon, L. Anderlucci, H. Alder, G. Nuovo, M. Li, M.V. Iorio, M. Galasso, R. Santhanam, G. Marcucci, D. Perrotti, K.A. Powell, A. Bratasz, M. Garofalo, K.P. Nephew, C.M. Croce, Estrogen mediated-activation of miR-191/425 cluster modulates tumorigenicity of breast cancer cells depending on estrogen receptor status, PLoS genetics, 9 (2013) e1003311.
[7] X. Tian, Z. Zhang, miR-191/DAB2 axis regulates the tumorigenicity of estrogen receptor-positive breast cancer, IUBMB life, 70 (2018) 71-80.
[8] N. Nagpal, R. Kulshreshtha, miR-191: an emerging player in disease biology, Front Genet, 5 (2014) 99.
[9] S. Volinia, G.A. Calin, C.G. Liu, S. Ambs, A. Cimmino, F. Petrocca, R. Visone, M. Iorio, C. Roldo, M. Ferracin, R.L. Prueitt, N. Yanaihara, G. Lanza, A. Scarpa, A. Vecchione, M. Negrini, C.C. Harris, C.M. Croce, A microRNA expression signature of human solid tumors defines cancer gene targets, Proceedings of the National Academy of Sciences of the United States of America, 103 (2006) 2257-2261.
[10] M.A. Chaudhry, R.A. Omaruddin, C.D. Brumbaugh, M.A. Tariq, N. Pourmand, Identification of radiation-induced microRNA transcriptome by next-generation massively parallel sequencing, Journal of radiation research, 54 (2013) 808-822.
[11] B. Li, X.B. Shi, D. Nori, C.K. Chao, A.M. Chen, R. Valicenti, V. White Rde, Down-regulation of microRNA 106b is involved in p21-mediated cell cycle arrest in response to radiation in prostate cancer cells, Prostate, 71 (2011) 567-574.
[12] N. Cancer Genome Atlas Research, The Molecular Taxonomy of Primary Prostate Cancer, Cell, 163 (2015) 1011-1025.
[13] M. Fraser, V.Y. Sabelnykova, T.N. Yamaguchi, L.E. Heisler, J. Livingstone, V. Huang, Y.J. Shiah, F. Yousif, X. Lin, A.P. Masella, N.S. Fox, M. Xie, S.D. Prokopec, A. Berlin, E. Lalonde, M. Ahmed, D. Trudel, X. Luo, T.A. Beck, A. Meng, J. Zhang, A. D'Costa, R.E. Denroche, H. Kong, S.M. Espiritu, M.L. Chua, A. Wong, T. Chong, M. Sam, J. Johns, L. Timms, N.B. Buchner, M. Orain, V. Picard, H. Hovington, A. Murison, K. Kron, N.J. Harding, C. P'ng, K.E. Houlahan, K.C. Chu, B. Lo, F. Nguyen, C.H. Li, R.X. Sun, R. de Borja, C.I. Cooper, J.F. Hopkins, S.K. Govind, C. Fung, D. Waggott, J. Green, S. Haider, M.A. Chan-Seng-Yue, E. Jung, Z. Wang, A. Bergeron, A. Dal Pra, L. Lacombe, C.C. Collins, C. Sahinalp, M. Lupien, N.E. Fleshner, H.H. He, Y. Fradet, B. Tetu, T. van der Kwast, J.D. McPherson, R.G. Bristow, P.C. Boutros, Genomic hallmarks of localized, non-indolent prostate cancer, Nature, 541 (2017) 359-364.

[14] S. Jain, C.A. Lyons, S.M. Walker, S. McQuaid, S.O. Hynes, D.M. Mitchell, B. Pang, G.E. Logan, A.M. McCavigan, D. O'Rourke, D.G. McArt, S.S. McDade, I.G. Mills, K.M. Prise, L.A. Knight, C.J. Steele, P.W. Medlow, V. Berge, B. Katz, D.A. Loblaw, D.P. Harkin, J.A. James, J.M. O'Sullivan, R.D. Kennedy, D.J. Waugh, Validation of a Metastatic Assay using biopsies to improve risk stratification in patients with prostate cancer treated with radical radiation therapy, Annals of oncology : official journal of the European Society for Medical Oncology, 29 (2018) 215-222.
[15] F.M. Frame, D. Pellacani, A.T. Collins, N.J. Maitland, Harvesting Human Prostate Tissue Material and Culturing Primary Prostate Epithelial Cells, Methods in molecular biology (Clifton, N.J.), 1443 (2016) 181-201.
[16] C. Lewis, S. McQuaid, P. Clark, P. Murray, T. McGuigan, C. Greene, B. Coulter, K. Mills, J. James, The Northern Ireland Biobank: A Cancer Focused Repository of Science, Open Journal of Bioresources, 5 (2018).
[17] X. Huang, S. Taeb, S. Jahangiri, U. Emmenegger, E. Tran, J. Bruce, A. Mesci, E. Korpela, D. Vesprini, C.S. Wong, R.G. Bristow, F.F. Liu, S.K. Liu, miRNA-95 mediates radioresistance in tumors by targeting the sphingolipid phosphatase SGPP1, Cancer research, 73 (2013) 6972-6986.
[18] H. Dweep, C. Sticht, P. Pandey, N. Gretz, miRWalk--database: prediction of possible miRNA binding sites by "walking" the genes of three genomes, Journal of biomedical informatics, 44 (2011) 839-847.
[19] J.N. Eskra, J.W. Kuiper, P.D. Walden, M.C. Bosland, N. Ozten, Interactive effects of 9-cis-retinoic acid and androgen on proliferation, differentiation, and apoptosis of LNCaP prostate cancer cells, European journal of cancer prevention : the official journal of the European Cancer Prevention Organisation (ECP), 26 (2017) 71-77.
[20] G.H. Windbichler, E. Hensler, M. Widschwendter, A. Posch, G. Daxenbichler, E. Fritsch, C. Marth, Increased radiosensitivity by a combination of 9-cis-retinoic acid and interferon-y in breast cancer cells, Gynecologic oncology, 61 (1996) 387-394.
[21] Y. He, Y. Cui, W. Wang, J. Gu, S. Guo, K. Ma, X. Luo, Hypomethylation of the hsa-miR-191 locus causes high expression of hsa-mir-191 and promotes the epithelial-to-mesenchymal transition in hepatocellular carcinoma, Neoplasia (New York, N.Y.), 13 (2011) 841-853.
[22] X. Wang, Z. Shi, X. Liu, Y. Su, W. Li, H. Dong, L. Zhao, M. Li, Y. Wang, X. Jin, Z. Huo, Upregulation of miR-191 promotes cell growth and invasion via targeting TIMP3 in prostate cancer, Journal of B.U.ON. : official journal of the Balkan Union of Oncology, 23 (2018) 444-452.
[23] K.R. Leite, A. Tomiyama, S.T. Reis, J.M. Sousa-Canavez, A. Sanudo, M.F. Dall'Oglio, L.H. Camara-Lopes, M. Srougi, MicroRNA-100 expression is independently related to biochemical recurrence of prostate cancer, The Journal of urology, 185 (2011) 1118-1122.
[24] H.J. Peltier, G.J. Latham, Normalization of microRNA expression levels in quantitative RT-PCR assays: identification of suitable reference RNA targets in normal and cancerous human solid tissues, RNA (New York, N.Y.), 14 (2008) 844-852.
[25] N. Nagpal, H.M. Ahmad, B. Molparia, R. Kulshreshtha, MicroRNA-191, an estrogen-responsive microRNA, functions as an oncogenic regulator in human breast cancer, Carcinogenesis, 34 (2013) 1889-1899.
[26] N. Nagpal, H.M. Ahmad, S. Chameettachal, D. Sundar, S. Ghosh, R. Kulshreshtha, HIF-inducible miR-191 promotes migration in breast cancer through complex regulation of TGFbeta-signaling in hypoxic microenvironment, Scientific reports, 5 (2015) 9650.
[27] S. Sharma, N. Nagpal, P.C. Ghosh, R. Kulshreshtha, P53-miR-191-SOX4 regulatory loop affects apoptosis in breast cancer, RNA (New York, N.Y.), 23 (2017) 1237-1246.
[28] A. Jacobsen, J. Silber, G. Harinath, J.T. Huse, N. Schultz, C. Sander, Analysis of microRNA-target interactions across diverse cancer types, Nature Structural &Amp; Molecular Biology, 20 (2013) 1325.
[29] A.A. Svoronos, D.M. Engelman, F.J. Slack, OncomiR or Tumor Suppressor? The Duplicity of MicroRNAs in Cancer, Cancer research, 76 (2016) 3666-3670.

[30] I.P. Uray, E. Dmitrovsky, P.H. Brown, Retinoids and rexinoids in cancer prevention: from laboratory to clinic, Semin Oncol, 43 (2016) 49-64.
[31] D.L. McCormick, K.V. Rao, V.E. Steele, R.A. Lubet, G.J. Kelloff, M.C. Bosland, Chemoprevention of rat prostate carcinogenesis by 9-cis-retinoic acid, Cancer research, 59 (1999) 521-524.
[32] F.F. Kabbinavar, N. Zomorodian, M. Rettig, F. Khan, D.R. Greenwald, S.J. Davidson, B.A. DiCarlo, R. Patel, L. Pandit, R. Chandraratna, M. Sanders, An open-label phase II clinical trial of the RXR agonist IRX4204 in taxane-resistant, castration-resistant metastatic prostate cancer (CRPC), Journal of Clinical Oncology, 32 (2014) 5073-5073.
[33] C. Zhong, S. Yang, J. Huang, M.B. Cohen, P. Roy-Burman, Aberration in the expression of the retinoid receptor, RXRalpha, in prostate cancer, Cancer biology & therapy, 2 (2003) 179-184.

Table I. hPCA9 clinical characteristics.

INITIAL DIAGNOSIS						RELAPSE		
Date	**Age**	**PSA**	**Gleason score**	**TNM Stage**	**Treatment**	**Date**	**Age**	**PSA**
2009	57	19	3+4	T1cN0M0	Bicalutamide & 60Gy/20 EBRT	2017	65	3.84

Figure 1: miR-191 abundance in prostate cancer.

(A) miR-191 abundance is significantly higher in tumor (n=487) vs normal (n=52) prostate tissue samples from the TCGA cohort. (B) In the TCGA dataset, increased abundance of miR-191 is observed in higher Gleason scores (ANOVA, $p=6.3 \times 10^{-4}$). (C) Kaplan-Meier plot of biochemical-free survival rate (BCR) in 50 CPC-GENE patients treated with radical prostatectomy with time to relapse < 5 years, stratified by miR-191 abundance (HR=1.61).

Figure 2: miR-191 overexpression results in increased radiation resistance *in vitro*.

(A) Radiation survival curves from clonogenic assays performed using DU145 and PC3 cells transfected with either control or miR-191 mimic. Survival curves represent linear quadratic regression of surviving fraction. (B) Viable cell counts of DU145 cells transiently transfected with control or miR-191 mimic, and treated with no radiation (Mock IR) or 6Gy irradiated (+IR). Data graphed as fold change in number of viable cells at day 4 (Mock IR) and day 5 (+IR). (C) Cell cycle profile of DU145 cells transfected with control or miR-191 mimic, assessed 24 hours after mock irradiation (left) or irradiated (10Gy, right). (D) Viable cell counts and (E) cell cycle profile of PC3 cells transiently transfected with control or miR-191 mimic, and treated with mock irradiation or irradiated. Data represented as mean ± SEM, statistical significance denoted (* $p<0.05$, ** $p<0.01$, *** $p<0.001$, ns=not significant).

Figure 3: RXRA is a direct target of miR-191.

(A) Flowchart of approach used to identify targets of miR-191 in prostate cancer. Data from transcriptomic array in DU145 cells transfected with miR-191 or control mimic was combined with *in silico* predicted targets based on miR-191 target sequence. (B) qRT-PCR and western blot examining *RXRA* abundance in DU145 and PC3 cells with control or miR-191 mimic transient transfection. qRT-PCR normalized to *GAPDH*, n=4 biological replicates. Representative western blot images shown. (C) Firefly luciferase activity in DU145 cells transiently transfected with wild-type (WT) or mutated (MT) RXRA 3'UTR luciferase vector, in combination with control or miR-191 mimic. Single representative experiment shown. Activity normalized to B-gal reporter control.

Figure 4: Low RXRA prostate cancer abundance is associated with worse patient outcomes.

(A) Prostate tumors from the TCGA dataset exhibit lower RXRA abundance compared with normal prostate tissue. (B) Kaplan-Meier plot of CPC-GENE patient cohort showing biochemical relapse-free survival rate (BCR) stratified by RXRA abundance (HR=0.56). (C) Combined Kaplan-Meier plot with biochemical relapse-free survival rate stratified by miR-191 and RXRA abundance in CPC-GENE cohort. (D) Kaplan-Meier plot of Belfast prostate cancer cohort showing metastatic-free survival stratified by RXRA abundance.

Figure 5: miR-191 mediates radioresistance through RXRA, in established and primary prostate cancer cell line hPCA9.

(A) Radiation clonogenic survival curves and (B) viable cell results of DU145 and PC3 cells transfected with control or RXRA siRNA. (C) Surviving fraction after 8Gy (IR) of DU145 cells transfected with control or miR-191 mimic and treated with DMSO or 1µM 9cRA prior to IR. (D) Clonogenic survival of hPCA9 cells transfected with miR-191 mimic (left) or RXRA siRNA (right). (E) Surviving fraction at 6Gy of hPCA9 cells pretreated with DMSO or 0.1µM 9cRA prior to IR. Data represented as mean ± SEM, statistical significance denoted (* $p<0.05$, ** $p<0.01$, ns=not significant).

Figure 6: miR-191 promotes radiation resistance *in vivo*.

(A) Radiation clonogenic survival (left) and viable cell counts (right) of DU145 cells with stable miR-191 (miR-191-st) or control (control-st) overexpression. (B) DU145 control and miR-191 stable tumors treated with mock irradiation (Mock IR) or 6Gy (+IR) at Day 0. Tumor volume normalized to starting volume at Day 0. (C) H&E staining for tumor necrosis and (D) immunohistochemistry staining for the proliferative marker Ki-67 in DU145 control-st and miR-191-st tumor sections treated with 6Gy radiation (+IR), representative sections shown on the right. Necrotic area relative to total tumor area. Data represented as mean ± SEM, statistical significance denoted (* $p<0.05$, ** $p<0.01$, ns=not significant).

Supplementary Figure 1: Transfection efficiencies. (A) qRT-PCR results confirming transient overexpression of miR-191 with mimic transfection, and (B) RXRA knockdown at mRNA and protein level by RXRA siRNA transfection in DU145, PC3, and hPCA9 cells. (C) miR-191 mimic reduces RXRA mRNA in hPCA9 cells following transfection. (D) Consistent overexpression in miR-191 stable DU145 cells compared with control DU145 cells, as determined by qRT-PCR. Data represented as mean ± SEM.

Supplementary Figure 2: EdU cell cycle profiles. (A) DU145 cells and (B) PC3 cells transfected with control or miR-191 mimic, treated with Mock (0Gy) or 10Gy radiation, and pulsed 24 hours later with EdU.

Supplementary Figure 3: Full clonogenic survival curves after 9cRA treatment. Surviving fraction of DU145 (left) or hPCA9 (right) cells treated with 1µM (DU145) or 0.1µM (hPCA9) 9cRA or matched DMSO. DU145 curve performed using cells transiently transfected with control or miR-191 mimic, then treated with 9cRA or vehicle. Data represented as mean ± SEM.

Supplementary Figure 4: γH2AX foci resolution following irradiation. DU145 cells transfected with control or miR-191 mimic were treated with Mock (0Gy) or 10Gy radiation, followed by flow-cytometry for detection of γH2AX foci.

Figure 1

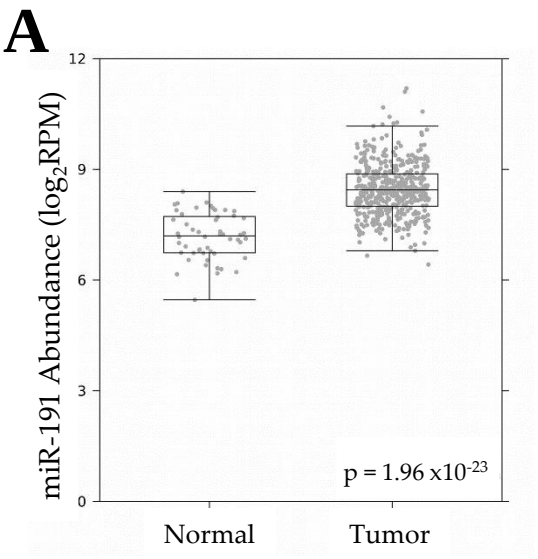

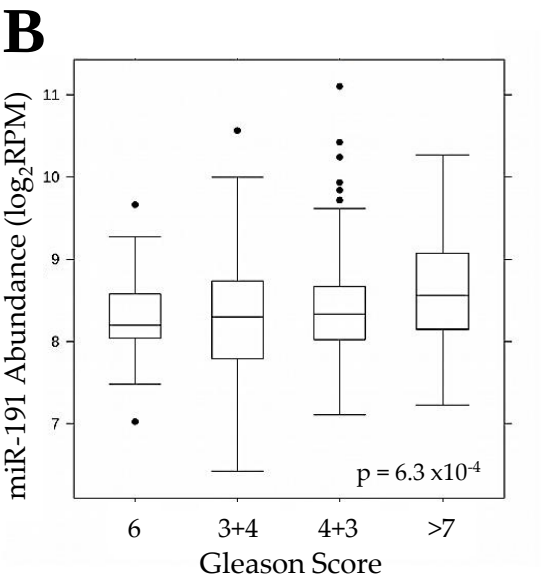

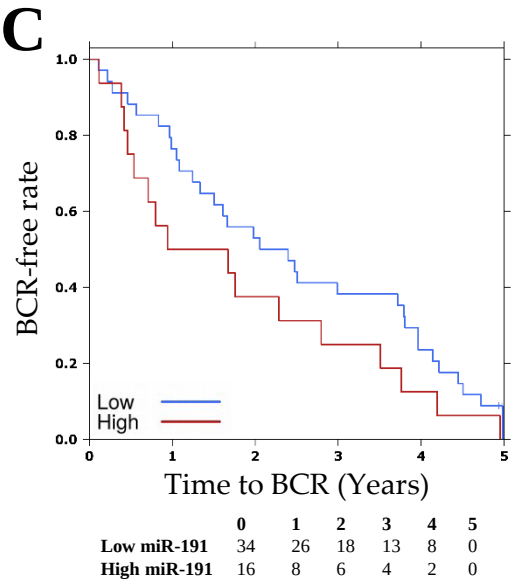

	0	1	2	3	4	5
Low miR-191	34	26	18	13	8	0
High miR-191	16	8	6	4	2	0

Figure 2

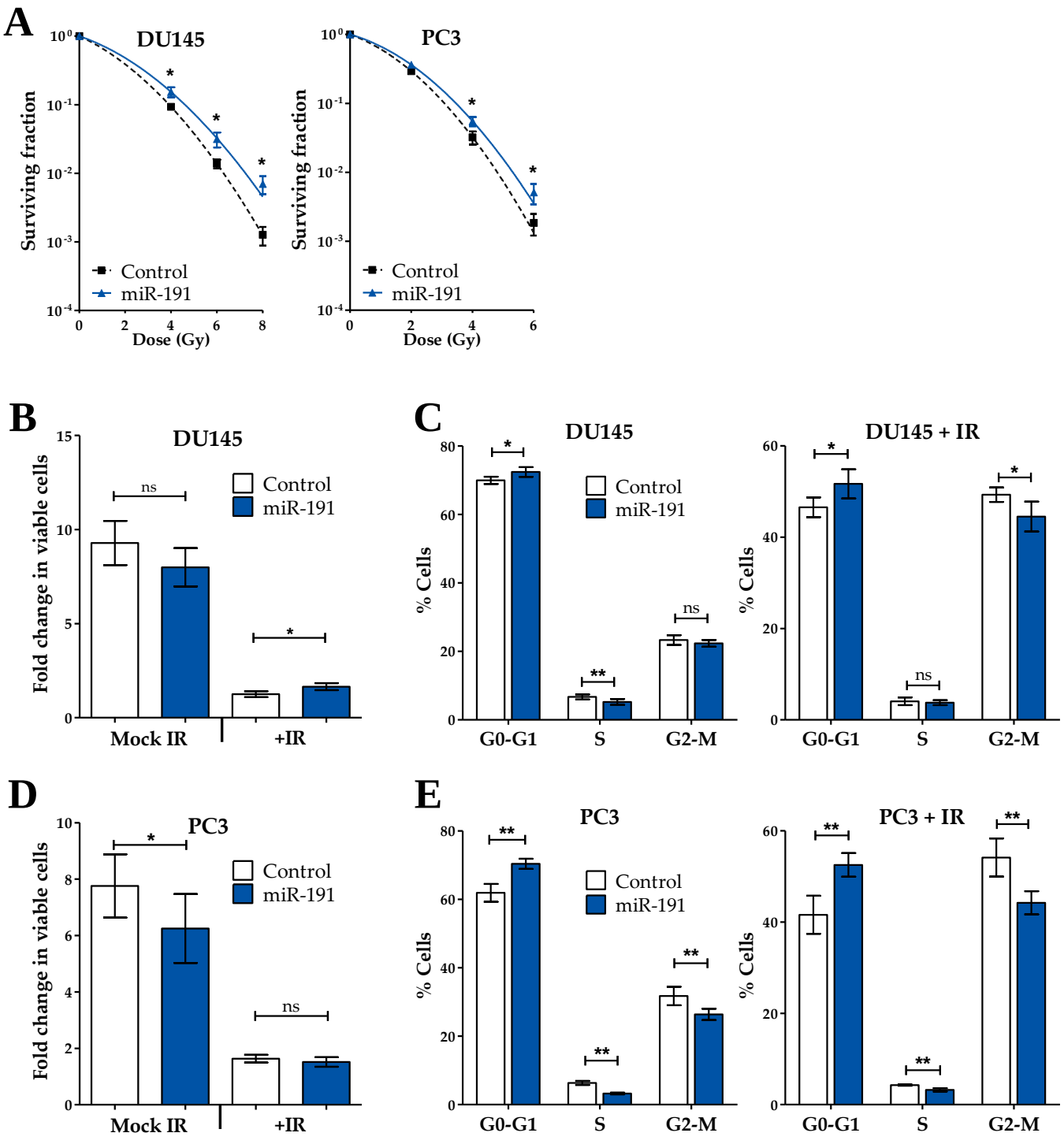
A
DU145
PC3
Surviving fraction
Dose (Gy)
Control
miR-191
B
DU145
Fold change in viable cells
ns
Mock IR
+IR
C
DU145
DU145 + IR
% Cells
G0-G1
S
G2-M
D
PC3
E
PC3
PC3 + IR

Figure 3

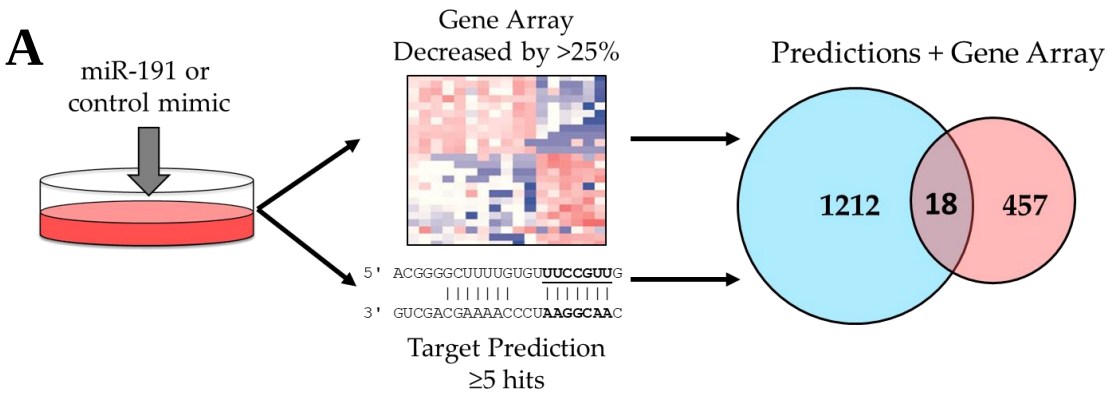

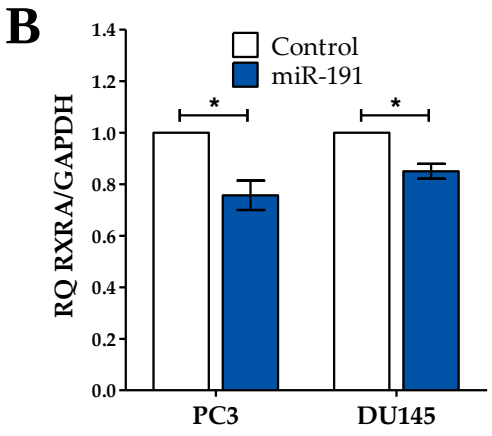

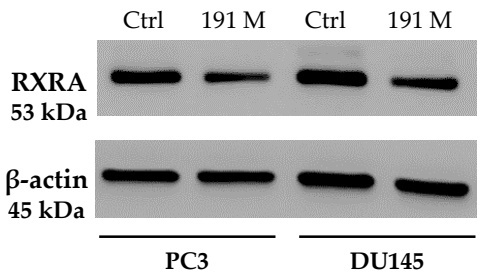

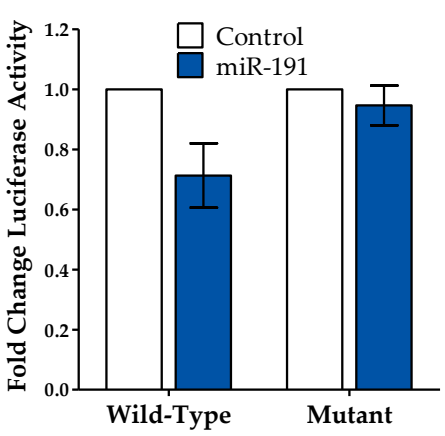

5' ACGGGGCUUUUGUGUUUCCGUUG RXRA WT 3'UTR
3' GUCGACGAAAACCCUAAGGCAAC miR-191
5' ACGGGGCUUUUGUGUAAGGCAAC RXRA MT 3'UTR

Figure 4

A

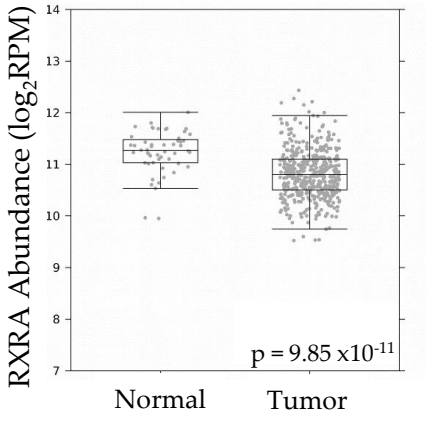

B

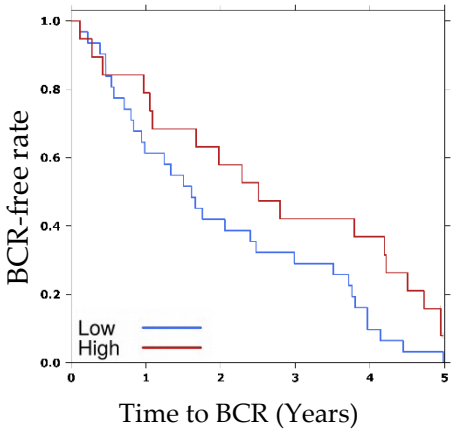

	0	1	2	3	4	5
Low RXRA	31	19	13	9	3	0
High RXRA	19	15	11	8	7	0

C

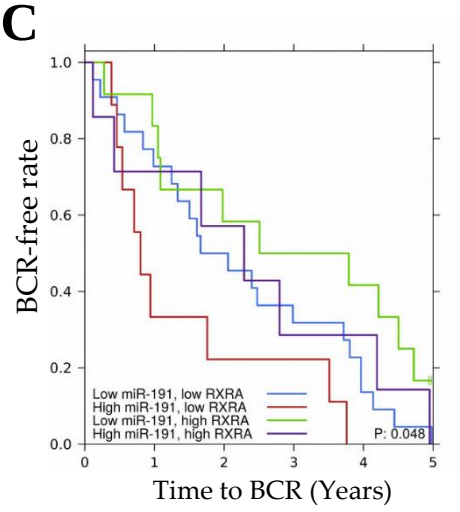

	0	1	2	3	4	5
Low miR-191, low RXRA	22	16	11	7	3	0
High miR-191, low RXRA	9	3	2	2	0	0
Low miR-191, high RXRA	12	10	7	6	5	0
High miR-191, high RXRA	7	5	4	2	2	0

D

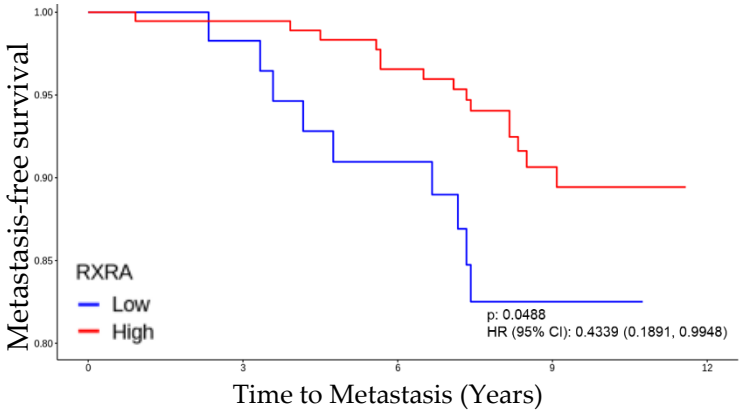

	0	3	6	9	12
Low RXRA	62	55	47	12	0
High RXRA	186	180	163	78	0

Figure 5

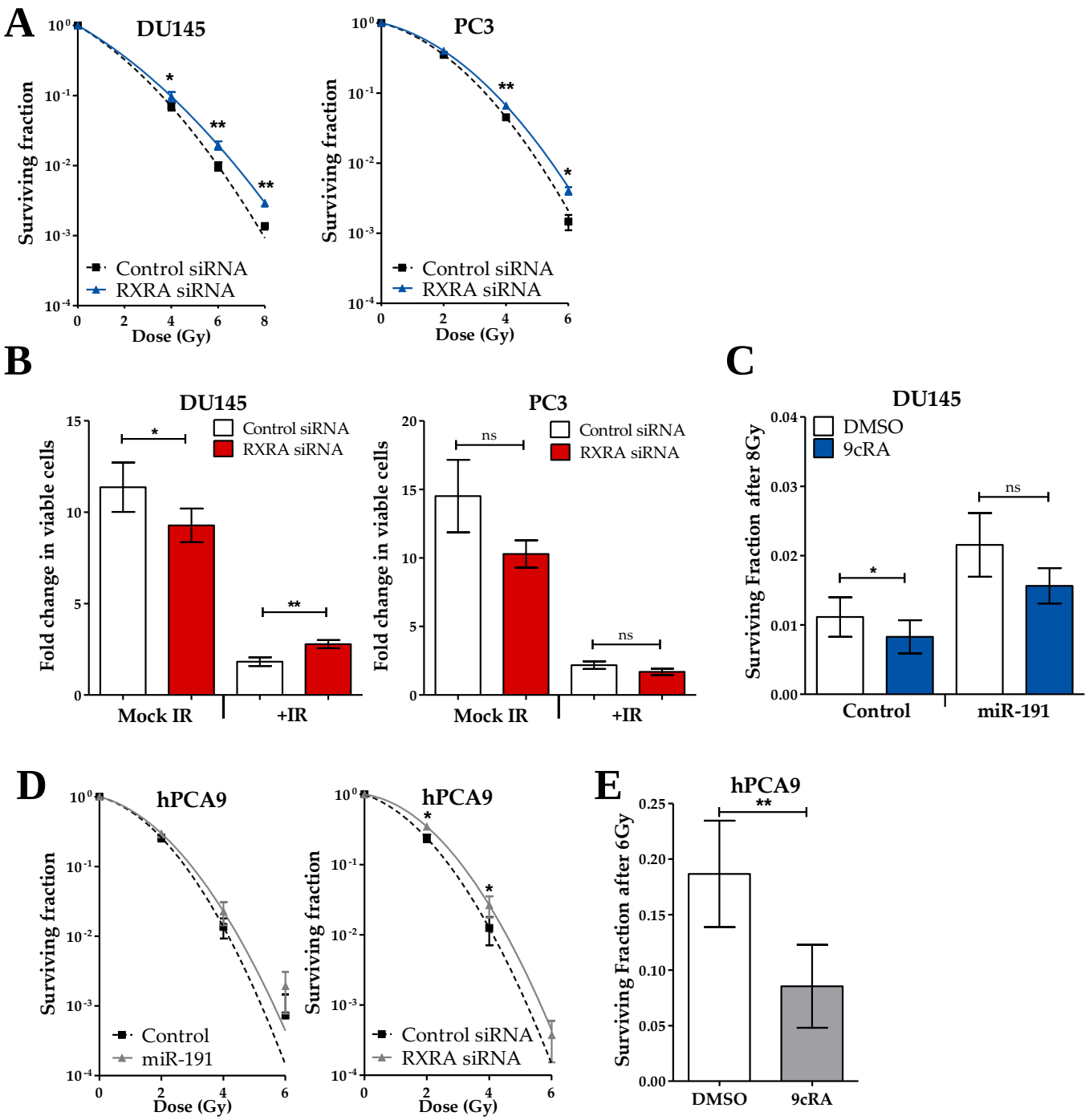
A
DU145
PC3
Surviving fraction
Dose (Gy)
Control siRNA
RXRA siRNA
B
DU145
PC3
Fold change in viable cells
Mock IR
+IR
ns
C
DU145
DMSO
9cRA
Surviving Fraction after 8Gy
Control
miR-191
D
hPCA9
Control
miR-191
Control siRNA
RXRA siRNA
E
hPCA9
Surviving Fraction after 6Gy
DMSO
9cRA

Figure 6

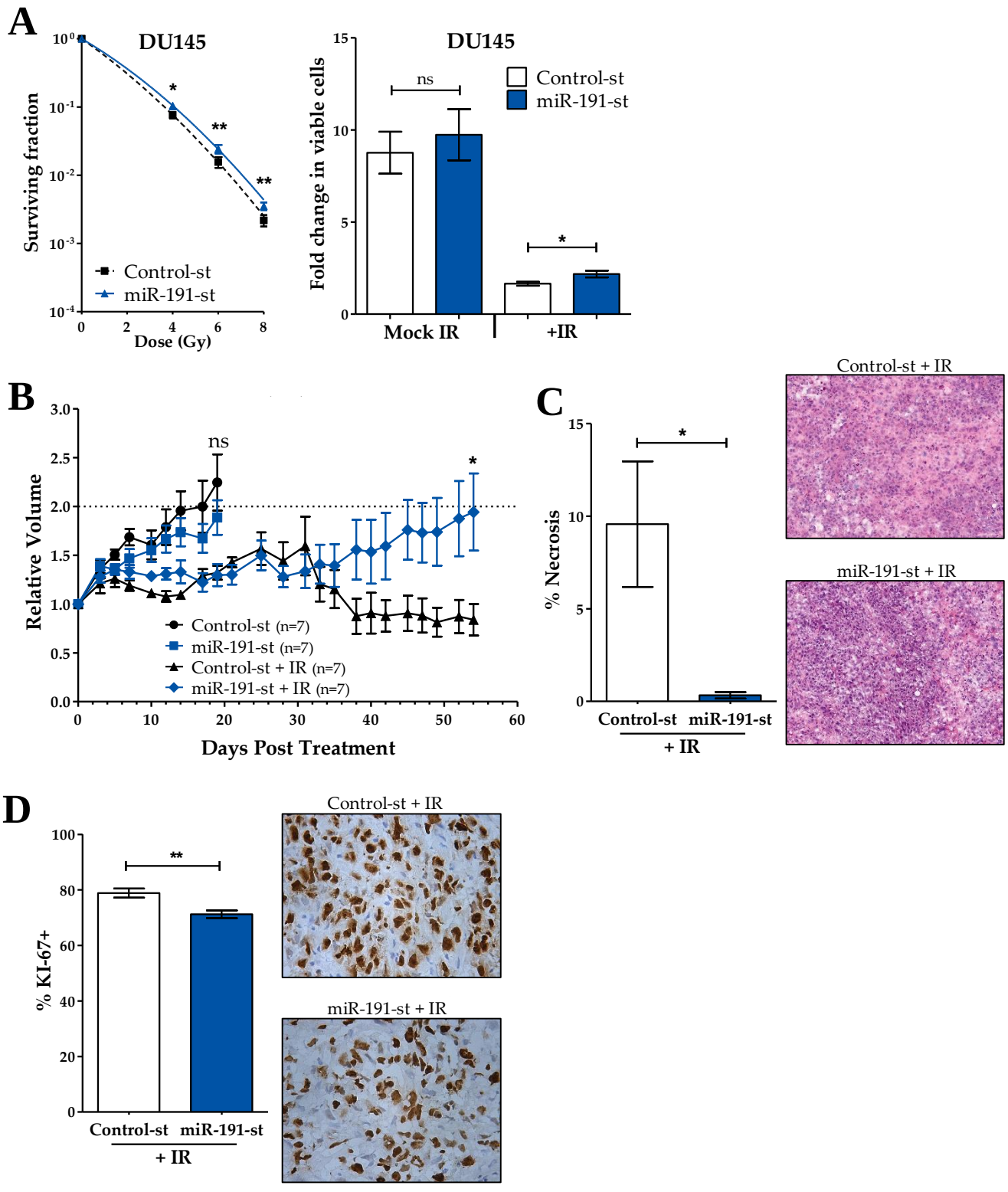
A
DU145
Surviving fraction
Dose (Gy)
Control-st
miR-191-st
DU145
Fold change in viable cells
ns
Control-st
miR-191-st
Mock IR
+IR
B
Relative Volume
Days Post Treatment
Control-st (n=7)
miR-191-st (n=7)
Control-st + IR (n=7)
miR-191-st + IR (n=7)
C
% Necrosis
Control-st
miR-191-st
+ IR
Control-st + IR
miR-191-st + IR
D
% KI-67+
Control-st
miR-191-st
+ IR
Control-st + IR
miR-191-st + IR

Highlights

- miR-191 expression is elevated in prostate cancer patients with higher Gleason score
- High miR-191 promotes radiation survival and targets retinoid X receptor alpha, RXRA
- Treatment with the RXRA agonist 9-cis-retinoic acid restores radiosensitivity
- Patients with high miR-191 and low RXRA experienced quicker biochemical recurrence

Conflict of Interest Statement: No conflicts of interest to declare.